J|A|C|S
ARTICLES
Published on Web 01/03/2007

Synthesis, Characterization, and Reactivities of Manganese(V)−Oxo Porphyrin Complexes

Woon Ju Song,[†] Mi Sook Seo,[†] Serena DeBeer George,[‡] Takehiro Ohta,[||] Rita Song,[†] Min-Jung Kang,[†] Takehiko Tosha,[||] Teizo Kitagawa,[||] Edward I. Solomon,[§] and Wonwoo Nam*,[†]

Contribution from the Department of Chemistry, Division of Nano Sciences, and Center for Biomimetic Systems, Ewha Womans University, Seoul 120-750, Korea, Stanford Synchrotron Radiation Laboratory, SLAC, Stanford University, Stanford, California 94309, Okazaki Institute for Integrative Bioscience, National Institutes of Natural Sciences, Okazaki, Aichi 444-8787, Japan, and Department of Chemistry, Stanford University, Stanford, California 94305

Received September 7, 2006; E-mail: wwnam@ewha.ac.kr

Abstract: The reactions of manganese(III) porphyrin complexes with terminal oxidants, such as *m*-chloroperbenzoic acid, iodosylarenes, and H_2O_2, produced high-valent manganese(V)−oxo porphyrins in the presence of base in organic solvents at room temperature. The manganese(V)−oxo porphyrins have been characterized with various spectroscopic techniques, including UV−vis, EPR, ^{1}H and ^{19}F NMR, resonance Raman, and X-ray absorption spectroscopy. The combined spectroscopic results indicate that the manganese(V)−oxo porphyrins are diamagnetic low-spin ($S = 0$) species with a longer, weaker Mn−O bond than in previously reported Mn(V)−oxo complexes of non-porphyrin ligands. This is indicative of double-bond character between the manganese(V) ion and the oxygen atom and may be attributed to the presence of a trans axial ligand. The $[(Porp)Mn^{V}{=}O]^{+}$ species are stable in the presence of base at room temperature. The stability of the intermediates is dependent on base concentration. In the absence of base, $(Porp)Mn^{IV}{=}O$ is generated instead of the $[(Porp)Mn^{V}{=}O]^{+}$ species. The stability of the $[(Porp)Mn^{V}{=}O]^{+}$ species also depends on the electronic nature of the porphyrin ligands: $[(Porp)Mn^{V}{=}O]^{+}$ complexes bearing electron-deficient porphyrin ligands are more stable than those bearing electron-rich porphyrins. Reactivity studies of manganese(V)−oxo porphyrins revealed that the intermediates are capable of oxygenating PPh_3 and thioanisoles, but not olefins and alkanes at room temperature. These results indicate that the oxidizing power of $[(Porp)Mn^{V}{=}O]^{+}$ is low in the presence of base. However, when the $[(Porp)Mn^{V}{=}O]^{+}$ complexes were associated with iodosylbenzene in the presence of olefins and alkanes, high yields of oxygenated products were obtained in the catalytic olefin epoxidation and alkane hydroxylation reactions. Mechanistic aspects, such as oxygen exchange between $[(Porp)Mn^{V}{=}^{16}O]^{+}$ and $H_2{}^{18}O$, are also discussed.

Introduction

An important objective in understanding biological oxidation by heme-containing monooxygenases is to elucidate the nature of the reactive intermediates and the mechanism of oxygen atom transfer from the intermediates to organic substrates.[1] Since the catalytic cycle of cytochrome P450 (CYP 450) is believed to involve a high-valent iron(IV)−oxo porphyrin π-cation radical, $[(Porp)^{+\bullet}Fe^{IV}{=}O]^{+}$, as an active oxidant in oxidation reactions,[2] a number of iron(IV)−oxo porphyrin π-cation radicals have been synthesized by the reaction of iron(III) porphyrins with terminal oxidants such as *m*-chloroperbenzoic acid (*m*-CPBA) and iodosylarenes (ArIO), characterized with various spectroscopic techniques, and studied in a variety of oxidation reactions, including alkane hydroxylation and olefin epoxidation.[3,4]

Synthetic manganese(III) porphyrins have also been extensively studied as CYP 450 models in oxygen-atom-transfer

[†] Ewha Womans University.
[‡] Stanford Synchrotron Radiation Laboratory.
[||] Okazaki Institute for Integrative Bioscience.
[§] Stanford University.

(1) (a) Ortiz de Montellano, P. R. *Cytochrome P450: Structure, Mechanism, and Biochemistry*, 3rd ed.; Kluwer Academic/Plenum Publishers: New York, 2005. (b) Denisov, I. G.; Makris, T. M.; Sligar, S. G.; Schlichting, I. *Chem. Rev.* **2005**, *105*, 2253−2278. (c) Meunier, B.; de Visser, S. P.; Shaik, S. *Chem. Rev.* **2004**, *104*, 3947−3980. (d) Groves, J. T. *Proc. Natl. Acad. Sci. U.S.A.* **2003**, *100*, 3569−3574. (e) Ortiz de Montellano, P. R.; De Voss, J. J. *Nat. Prod. Rep.* **2002**, *19*, 477−493.
(2) (a) Kellner, D. G.; Hung, S.-C.; Weiss, K. E.; Sligar, S. G. *J. Biol. Chem.* **2002**, *277*, 9641−9644. (b) Schlichting, I.; Berendzen, J.; Chu, K.; Stock, A. M.; Maves, S. A.; Benson, D. E.; Sweet, R. M.; Ringe, D.; Petsko, G. A.; Sligar, S. G. *Science* **2000**, *287*, 1615−1622. (c) Egawa, T.; Shimada, H.; Ishimura, Y. *Biochem. Biophys. Res. Commun.* **1994**, *201*, 1464−1469.
(3) (a) Nam, W. In *Comprehensive Coordination Chemistry II: From Biology to Nanotechnology*; Que, L., Jr., Tolman, W. T., Eds.; Elsevier Ltd.: Oxoford, 2004; Vol. 8, pp 281−307. (b) Fujii, H. *Coord. Chem. Rev.* **2002**, *226*, 51−60. (c) McLain, J. L.; Lee, J.; Groves, J. T. In *Biomimetic Oxidations Catalyzed by Transition Metal Complexes*; Meunier, B., Ed.; Imperial College Press: London, 2000; pp 91−169. (d) Watanabe, Y. In *The Porphyrin Handbook*, Vol. 4; Kadish, K. M., Smith, K. M., Guilard, R., Ed.; Academic: New York, 2000; Vol. 30, pp 97−117.
(4) (a) Groves, J. T.; Haushalter, R. C.; Nakamura, M.; Nemo, T. E.; Evans, B. J. *J. Am. Chem. Soc.* **1981**, *103*, 2884−2886. (b) Gross, Z.; Nimri, S. *Inorg. Chem.* **1994**, *33*, 1731−1732. (c) Gross, Z.; Nimri, S.; Barzilay, C. M.; Simkhovich, L. *J. Biol. Inorg. Chem.* **1997**, *2*, 492−506. (d) Goh, Y. M.; Nam, W. *Inorg. Chem.* **1999**, *38*, 914−920. (e) Song, W. J.; Ryu, Y. O.; Song, R.; Nam, W. *J. Biol. Inorg. Chem.* **2005**, *10*, 294−304.

 10.1021/ja066460v CCC: $37.00

reactions.[5] Although manganese porphyrins have shown promise as versatile catalysts in oxidation reactions over the past two decades, only recently have the key manganese(V)−oxo porphyrin intermediates been isolated, spectroscopically characterized, and studied in oxidation reactions.[6−9] Groves and co-workers reported the generation and characterization of the first manganese(V)−oxo porphyrin complexes in aqueous solution and the reactivities of these complexes in olefin epoxidation and in the oxidation of bromide and nitrite ions.[6] Subsequently, Nam and co-workers demonstrated that a manganese(V)−oxo porphyrin can be generated with a biologically relevant oxidant, H_2O_2, in aqueous solution and that the formation of the intermediate depends markedly on the pH of the reaction solutions.[7] Very recently, Newcomb and co-workers reported the generation of manganese(V)−oxo complexes via laser flash photolysis methods in organic solvents and the kinetic studies of the intermediates in olefin epoxidation and alkane hydroxylation.[8] Naruta and co-workers synthesized a dinuclear Mn^V═O porphyrin complex in the presence of base in organic solvents that showed O_2 evolution via O−O bond formation between the manganese(V)−oxo moieties.[9] In addition to the manganese(V)−oxo porphyrins, manganese(V)−oxo complexes bearing non-porphyrinic macrocycles, such as corrole and corrolazine, have been isolated and characterized.[10−15] Interestingly, the manganese(V)−oxo complexes of non-porphyrin ligands are very stable at room temperature and are poor oxidants in oxygen-atom-transfer reactions. Thus, insight into the chemical properties of the long-sought manganese(V)−oxo intermediates has been obtained by recent developments in isolating and characterizing manganese(V)−oxo complexes of porphyrin and non-porphyrin ligands. In this paper, we report the generation and characterization of manganese(V)−oxo porphyrin complexes that are stable at room temperature in the presence of base in organic solvents. The stability and reactivities of the manganese(V)−oxo porphyrins have been investigated in detail in oxygenation reactions under stoichiometric and catalytic conditions.

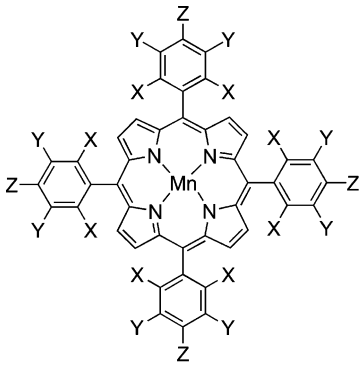

Mn(III) porphyrins	X	Y	Z
Mn(TDCPP)Cl	Cl	H	H
Mn(TDFPP)Cl	F	H	H
Mn(TPFPP)Cl	F	F	F
Mn(TMP)Cl	CH_3	H	CH_3
Mn(TDMPP)Cl	CH_3	H	H

Figure 1. Structure of manganese(III) porphyrin complexes used in this study.

Results and Discussion

Preparation and Characterization of Manganese(V)−Oxo Porphyrin Complexes. Addition of *m*-chloroperbenzoic acid (*m*-CPBA) to a reaction solution containing a manganese(III) porphyrin chloride, Mn(TDCPP)Cl (see Figure 1 for the structures of manganese porphyrin complexes used in this study),[16] and tetrabutylammonium hydroxide (TBAH) in a solvent mixture of CH_2Cl_2 and CH_3CN (1:1) at 25 °C resulted in the immediate generation of a manganese(V)−oxo porphyrin complex, $[(TDCPP)Mn^V{=}O]^+$ (**1a**), with a strong and sharp Soret band at 444 nm and a Q-band at 560 nm (Figure 2a; see Supporting Information, Figure S1 for UV−vis spectra of other manganese(V)−oxo porphyrins; Table 1 summarizes the UV−vis absorption bands).[6−9] The intermediate persisted for several hours ($t_{1/2} \approx 40$ min) at 35 °C. The formation of **1a** was also observed when Mn(TDCPP)Cl was treated with other oxidants, such as iodosylarenes (i.e., PhIO and F_5PhIO) and H_2O_2, under identical conditions.

The manganese(V)−oxo porphyrin complex **1a** was further characterized by EPR, ^{1}H and ^{19}F NMR, resonance Raman, and X-ray absorption spectroscopy. The X-band EPR of **1a** shows no signal (data not shown).[6b,7,9] The ^{1}H NMR spectrum of **1a** in CD_3CN displays sharp ^{1}H resonances in the normal aromatic region (δ 7−9 ppm) (Figure 2b). The β-pyrrole proton appears at 8.7 ppm as a sharp singlet, and the meta and para protons of the phenyl group appear at 7.9 and 8.1 ppm with an integral ratio of 2:1, respectively. Similarly, the ^{1}H NMR spectrum of $[(TDFPP)Mn^V{=}O]^+$ exhibits sharp signals for the β-pyrrole

(5) (a) Meunier, B. *Chem. Rev.* **1992**, *92*, 1411−1456. (b) Mansuy, D. *Coord. Chem. Rev.* **1993**, *125*, 129−141. (c) Groves, J. T. In *Cytochrome P450: Structure, Mechanism, and Biochemistry*, 3rd ed.; Ortiz de Montellano, P. R., Ed.; Kluwer Academic/Plenum Publishers: New York, 2005; pp 1−43.
(6) (a) Groves, J. T.; Lee, J.; Marla, S. S. *J. Am. Chem. Soc.* **1997**, *119*, 6269−6273. (b) Jin, N.; Groves, J. G. *J. Am. Chem. Soc.* **1999**, *121*, 2923−2924. (c) Jin, N.; Bourassa, J. L.; Tizio, S. C.; Groves, J. T. *Angew. Chem., Int. Ed.* **2000**, *39*, 3849−3851.
(7) Nam, W.; Kim, I.; Lim, M. H.; Choi, H. J.; Lee, J. S.; Jang, H. G. *Chem. Eur. J.* **2002**, *8*, 2067−2071.
(8) (a) Zhang, R.; Newcomb, M. *J. Am. Chem. Soc.* **2003**, *125*, 12418−12419. (b) Zhang, R.; Horner, J. H.; Newcomb, M. *J. Am. Chem. Soc.* **2005**, *127*, 6573−6582.
(9) Shimazaki, Y.; Nagano, T.; Takesue, H.; Ye, B.-H.; Tani, F.; Naruta, Y. *Angew. Chem., Int. Ed.* **2004**, *43*, 98−100.
(10) (a) Mandimutsira, B. S.; Ramdhanie, B.; Todd, R. C.; Wang, H.; Zareba, A. A.; Czernuszewicz, R. S.; Goldberg, D. P. *J. Am. Chem. Soc.* **2002**, *124*, 15170−15171. (b) Wang, S. H.; Mandimutsira, B. S.; Todd, R.; Ramdhanie, B.; Fox, J. P.; Goldberg, D. P. *J. Am. Chem. Soc.* **2004**, *126*, 18−19. (c) Lansky, D. E.; Mandimutsira, B.; Ramdhanie, B.; Clausén, M.; Penner-Hahn, J.; Zvyagin, S. A.; Telser, J.; Krzystek, J.; Zhan, R.; Ou, Z.; Kadish, K. M.; Zakharov, L.; Rheingold, A. L.; Goldberg, D. P. *Inorg. Chem.* **2005**, *44*, 4485−4498.
(11) (a) Golubkov, G.; Bendix, J.; Gray, H. B.; Mahammed, A.; Goldberg, I.; Dibilio, A. J.; Gross, Z. *Angew. Chem., Int. Ed.* **2001**, *40*, 2132−2134. (b) Gross, Z.; Golubkov, G.; Simkhovich, L. *Angew. Chem., Int. Ed.* **2000**, *39*, 4045−4047.
(12) Liu, H.-Y.; Lai, T.-S.; Yeung, L.-L.; Chang, C. K. *Org. Lett.* **2003**, *5*, 617−620.
(13) Zhang, R.; Harischandra, D. N.; Newcomb, M. *Chem. Eur. J.* **2005**, *11*, 5713−5720.
(14) (a) Miller, C. G.; Gordon-Wylie, S. W.; Horwitz, C. P.; Strazisar, S. A.; Peraino, D. K.; Clark, G. R.; Weintraub, S. T.; Collins, T. J. *J. Am. Chem. Soc.* **1998**, *120*, 11540−11541. (b) Workman, J. M.; Powell, R. D.; Procyk, A. D.; Collins, T. J.; Bocian, D. F. *Inorg. Chem.* **1992**, *31*, 1548−1550. (c) Collins, T. J.; Powell, R. D.; Slebodnick, C.; Uffelman, E. S. *J. Am. Chem. Soc.* **1990**, *112*, 899−901. (d) Collins, T. J.; Gordon-Wylie, S. W. *J. Am. Chem. Soc.* **1989**, *111*, 4511−4513.
(15) MacDonnell, F. M.; Fackler, N. L. P.; Stern, C.; O'Halloran, T. V. *J. Am. Chem. Soc.* **1994**, *116*, 7431−7432.

(16) Abbreviations: TDCPP, *meso*-tetrakis(2,6-dichlorophenyl)porphinato dianion; TDFPP, *meso*-tetrakis(2,6-difluorophenyl)porphinato dianion; TPFPP, *meso*-tetrakis(pentafluorophenyl)porphinato dianion; TMP, *meso*-tetramesitylporphinato dianion; TDMPP, *meso*-tetrakis(2,6-dimethylphenyl)-porphinato dianion; TM-2-PyP, *meso*-tetrakis(*N*-methyl-2-pyridyl)porphinato dianion.

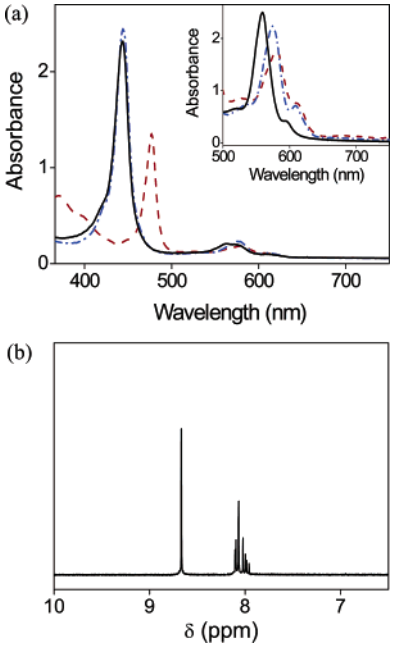

Figure 2. (a) UV−vis spectra of Mn(TDCPP)Cl (0.15 mM) (red dashed line), Mn(TDCPP)Cl (0.15 mM) in the presence of TBAH (3 mM) (blue dotted line), and **1a** (0.15 mM) (black solid line). Inset shows a magnification of the Q-band region of the manganese porphyrins (1.5 mM). (b) ^{1}H NMR spectrum of **1a**. **1a** was prepared by reacting Mn(TDCPP)Cl (1.5 mM) with H_2O_2 (3 mM) in the presence of TBAH (30 mM) in CD_3CN at ambient temperature. Chemical shifts (in ppm) were referenced to TMS (δ = 0.0 ppm).

Table 1. UV−Vis Absorption Bands and Rate Constants for the Natural Decay of [(Porp)Mn^V=O]$^+$ Complexes

	absorption bands		
(Porp)Mn^V=O	Soret band (nm), log ϵ	Q-bands (nm), log ϵ	rate of natural decay, k_{obs} (s^{-1})[a]
[(TPFPP)Mn^V=O]$^+$	434, 5.1(3)	553, 4.2(3)	1.3(2) × 10^{-4}
[(TDFPP)Mn^V=O]$^+$	436, 5.1(6)	552, 4.2(6)	1.9(3) × 10^{-4}
[(TDCPP)Mn^V=O]$^+$ (**1a**)	444, 5.1(6)	560, 4.1(4)	4.6(4) × 10^{-4}
[(TDMPP)Mn^V=O]$^+$	438, 5.1(5)	562, 4.0(6) 599, 3.8(3)	8.5(6) × 10^{-4}
[(TMP)Mn^V=O]$^+$	441, 5.1(3)	561, 4.0(4) 598, 3.7(4)	1.6(2) × 10^{-3}

[a] First-order rate constants, k_{obs}, were determined by monitoring absorbance changes of Q-bands of [(Porp)Mn^V=O]$^+$ (1.5 mM) in a 0.1-cm UV cell at 35 °C.

proton at 8.9 ppm and the meta and para protons of the phenyl group at 7.7 and 8.1 ppm with an integral ratio of 2:1, respectively (Supporting Information, Figure S2a). Further, the [(TDFPP)Mn^V=O]$^+$ complex shows a sharp ^{19}F NMR peak at −109 ppm for the phenyl fluorine (Supporting Information, Figure S2b).[11b,12] Such well-resolved signals in the ^{1}H and ^{19}F NMR spectra demonstrate that **1a** and other manganese(V)−oxo complexes are diamagnetic low-spin d^2 species.[6b,10b,11b,12]

Resonance Raman Analysis. The resonance Raman spectrum of **1a**, measured in CH_3CN at ambient temperature with 442-nm laser excitation, exhibited an isotope-sensitive band at 759 cm^{-1}, which shifted to 724 cm^{-1} when **1a**-^{18}O was generated with $H_2{}^{18}O_2$ or upon addition of $H_2{}^{18}O$ to the solution of **1a**-^{16}O (vide infra) (Figure 3a).[9] The observed isotopic shift by 35 cm^{-1} upon ^{18}O substitution is in good agreement with the value calculated ($\Delta\nu_{calc}$ = −34 cm^{-1}) from the Mn−O diatomic harmonic oscillator. Further, the observed Mn−O frequency at ∼759 cm^{-1} is consistent with double-bond

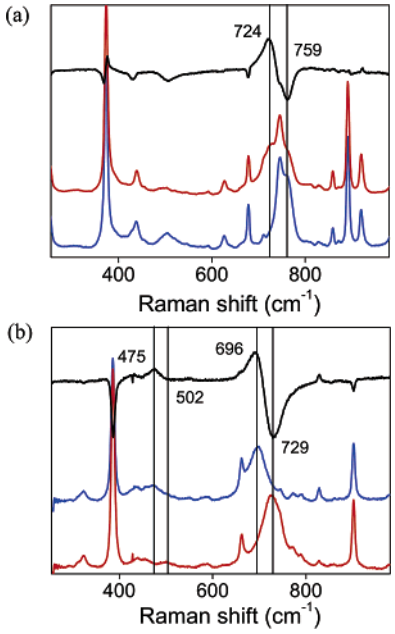

Figure 3. (a) Resonance Raman spectra of **1a**-^{16}O (blue line), **1a**-^{18}O (red line), and the difference between **1a**-^{16}O and **1a**-^{18}O (black line). (b) Resonance Raman spectra of [(TM-2-PyP)Mn^V=^{16}O]$^{5+}$ (red line), [(TM-2-PyP)Mn^V=^{18}O]$^{5+}$ (blue line), and the difference between [(TM-2-PyP)-Mn^V=^{16}O]$^{5+}$ and [(TM-2-PyP)Mn^V=^{18}O]$^{5+}$ (black line). See Experimental Section for detailed reaction procedures.

character between the manganese(V) ion and the oxygen atom (vide infra). Resonance Raman spectra were also obtained for [(TDFPP)Mn^V=O]$^+$ and [(TPFPP)Mn^V=O]$^+$. These data exhibit $\nu_{Mn=O}$ frequencies of 755 and 753 cm^{-1}, respectively, indicating that the Mn^V=O stretching frequency is not sensitive to the porphyrin ligand environment.[17] It is worth noting that the observed Mn^V=O stretching frequency of **1a** is lower than that of dinuclear (OH)Mn(V)=O species ($\nu_{Mn=O}$ = 791 cm^{-1})[9] but similar to that of Mn^{IV}(TMP)(O) ($\nu_{Mn=O}$ = 754 cm^{-1}).[18] In addition, when we prepared the manganese(V)−oxo porphyrin complex, [(TM-2-PyP)Mn^V=O]$^{5+}$,[16] in aqueous solution as reported by Groves and co-workers[6b,c] and measured the resonance Raman band of the Mn−O moiety, we observed a strong, isotope-sensitive band at 729 cm^{-1}, which shifted to 696 cm^{-1} when the manganese(V)−oxo porphyrin was generated in $H_2{}^{18}O$ (Figure 3b; see Supporting Information, Figure S3 for the UV−vis spectrum). A weak, isotope-sensitive band at 502 cm^{-1}, which shifted to 475 cm^{-1} upon introduction of ^{18}O, was also detected in the resonance Raman spectrum (Figure 3b). The bands at 729 and 502 cm^{-1} are assigned to ν(Mn^V=O) and ν(Mn^V−OH), respectively.[9] In contrast to the manganese(V)−oxo porphyrins, manganese(V)−oxo complexes bearing non-porphyrinic macrocycles exhibit a Mn−O stretching band at a higher frequency (e.g., ∼980 cm^{-1}) in organic solvents, which indicates triple-bond character between the Mn(V) ion and the oxo group.[10a,14b,c] The triple-bond character of Mn−O moieties in five-coordinate non-porphyrinic manganese(V)−oxo complexes has been confirmed by short Mn−O bond lengths

(17) It has been shown in iron porphyrin systems that the $\nu_{Fe=O}$ frequencies of high-valent iron(IV)−oxo porphyrin complexes are not sensitive to the overall oxidation state (i.e., $\Delta\nu_{Fe=O}$ of [(Porp)Fe^{IV}=O] and [(Porp)$^+$Fe^{IV}=O]$^+$ < 10 cm^{-1}) and the electronic nature of porphyrin ligands of the iron−oxo species: Kitagawa, T.; Mizutani, Y. *Coord. Chem. Rev.* **1994**, *135/136*, 685−735.

(18) Czernuszewicz, R. S.; Su, Y. O.; Stern, M. K.; Macor, K. A.; Kim, D.; Groves, J. T.; Spiro, T. G. *J. Am. Chem. Soc.* **1988**, *110*, 4158−4165.

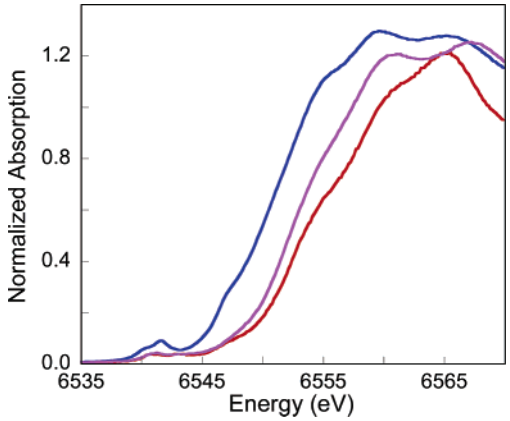

Figure 4. Comparison of the normalized Mn K-edge XAS data for the Mn^{III}(TDCPP)(OH) (blue), Mn^{IV}(TDCPP)(O) (purple), and [Mn^{V}(TDCPP)(O)]$^{+}$ (red) complexes.

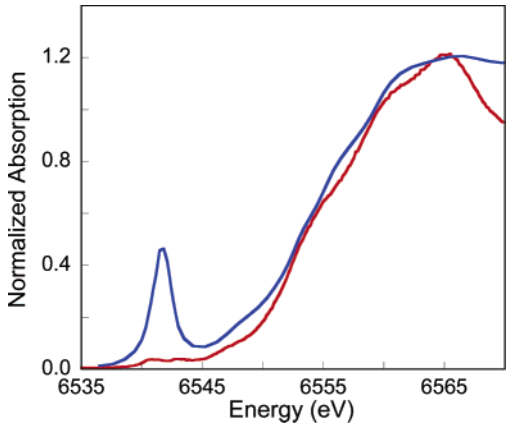

Figure 5. Comparison of the normalized Mn K-edge XAS data of the [Mn^{V}(TDCPP)(O)]$^{+}$ complex (red) to a five-coordinate [Mn^{V}(HMPAB)(O)]$^{-}$ complex (blue).

(~1.56 Å).[10c,14a,c,d,15] However, we have observed in the present study that the Mn−O stretching Raman bands of manganese(V)−oxo porphyrins are in the range of 760−790 cm^{-1} in organic solvents. This indicates a longer, weaker Mn−O bond, which suggests double-bond character.[9] The longer, weaker Mn−O bond (relative to known five-coordinate Mn(V)−oxo complexes) has been further confirmed by X-ray absorption spectroscopic studies, which suggest that the weakening of the Mn−O bond is due to the presence of a sixth ligand trans to the Mn−oxo bond (vide infra).

X-ray Absorption Spectroscopy (XAS)/Extended X-ray Absorption Fine Structure (EXAFS) Results. A comparison of the normalized Mn K-edge XAS data for the Mn(III)−, Mn(IV)−, and Mn(V)−TDCPP (**1a**) complexes is shown in Figure 4. The rising edge energy clearly increases across this series (increasing by ~2 eV upon oxidation of Mn(III) to Mn(IV), and by an additional ~1 eV on going to Mn(V)), consistent with the increasing effective nuclear charge on the manganese. Figure 5 shows a comparison of the normalized Mn K-edge XAS data for **1a** to those of the previously reported Na[Mn^{V}(HMPAB)(O)] (HMPAB = 1,2-bis(2-hydroxy-2-methylpropanamido)benzene) complex.[19] The rising edge positions are essentially identical, which thus confirms a Mn(V) oxidation state in the manganese porphyrin complex. However, the pre-edges (at ~6542 eV) of these two complexes are very different. The dramatic decrease in intensity requires an increased coordination number in **1a** compared to the five-coordinate Na[Mn^{V}(HMPAB)(O)] complex.[19] The presence of a strong trans axial ligand would weaken the Mn(V)−oxo bond (thus lowering $4p_z$ mixing) and would also shift the Mn more into the equatorial plane (lowering $4p_x$,p_y mixing), resulting in a more centrosymmetric Mn center. All of these factors contribute to a reduced electric dipole contribution and a weaker pre-edge intensity in **1a**,[20] compared to the previously reported five-coordinate Mn(V)−oxo complex.

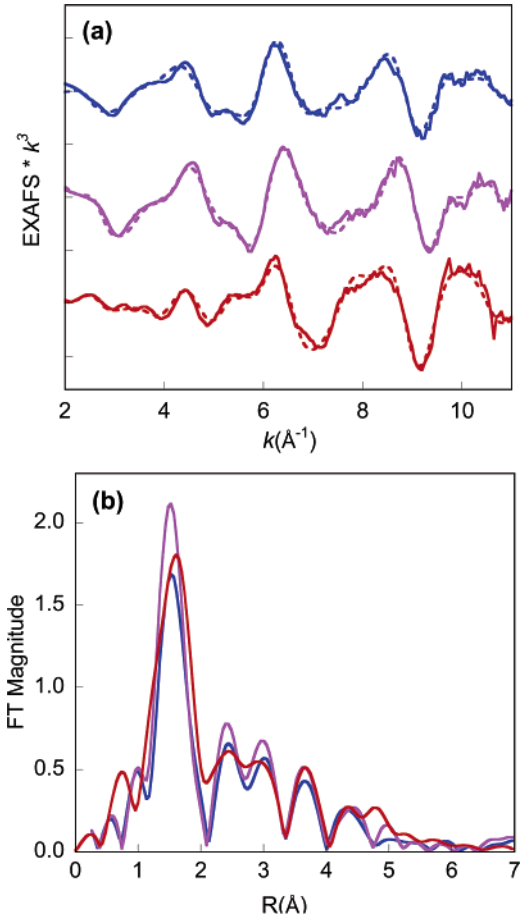

Figure 6. (a) Comparison of the EXAFS data (solid lines) and the fits to the data (dashed lines) for Mn^{III}(TDCPP)(OH) (blue), Mn^{IV}(TDCPP)(O) (purple), and [Mn^{V}(TDCPP)(O)]$^{+}$ (red). (b) The corresponding non-phase-shift-corrected Fourier transforms of the Mn^{III}(TDCPP)(OH) (blue), Mn^{IV}(TDCPP)(O) (purple), and [Mn^{V}(TDCPP)(O)]$^{+}$ (red) complexes.

The k^3-weighted EXAFS data and fits for the Mn(III)−, Mn(IV)−, and Mn(V)−TDCPP complexes are shown in Figure 6a. A comparison of the corresponding Fourier transforms (k = 2−11 Å^{-1}) is shown in Figure 6b. There are clear changes in the overall beat pattern of the EXAFS data and in the Fourier transforms upon oxidation. The best fits to the data are summarized in Table 2. For the Mn(III) complex, the EXAFS are best fit by inclusion of five Mn−N/O interactions at 2.01 Å, with additional outer-shell contributions from the porphyrin. Attempts to add a sixth ligand resulted in a slightly poorer fit (error increased from 0.45 to 0.54). Fits were also attempted in

(19) Weng, T.-C.; Hsieh, W.-Y.; Uffelman, E. S.; Gordon-Wylie, S. W.; Collins, T. J.; Pecoraro, V. L.; Penner-Hahn, J. E. *J. Am. Chem. Soc.* **2004**, *126*, 8070−8071.

(20) Westre, T. E.; Kennepohl, P.; DeWitt, J. G.; Hedman, B.; Hodgson, K. O.; Solomon, E. I. *J. Am. Chem. Soc.* **1997**, *119*, 6297−6314.

Table 2. EXAFS Fit Results

Mn(III)			Mn(IV)			Mn(V)		
	R (Å)	σ^2 (Å^2)		*R* (Å)	σ^2 (Å^2)		*R* (Å)	σ^2 (Å^2)
5 Mn−N/O	2.01	0.0036	6 Mn−N/O	1.99	0.0044	2 Mn−O	1.68	0.0051
						4 Mn−N	2.04	0.0023
8 Mn−C	3.04	0.0036	8 Mn−C	3.01	0.0036	8 Mn−C	3.06	0.0056
16 Mn−C−N	3.14	0.0100	16 Mn−C−N	3.15	0.0073	16 Mn−C−N	3.18	0.0080
4 Mn−C	3.44	0.0013	4 Mn−C	3.41	0.0034	4 Mn−C	3.45	0.0043
16 Mn−C−N	4.32	0.0079	16 Mn−C−N	4.31	0.0071	16 Mn−C−N	4.38	0.0068
ΔE_0	−4.61		ΔE_0	−0.92		ΔE_0	−0.56	
error[a]	0.45		error[a]	0.44		error[a]	0.60	

[a] Error is given by $\Sigma[(\chi_{obsd} - \chi_{calcd})^2 k^6]/\Sigma[(\chi_{obsd}^2 k^6]$.

which the first shell was split into shorter and longer components; however, this resulted in the two distances coalescing to the same value. The EXAFS results are consistent with the Mn(III) complex having an axial hydroxide ligand.

The Mn(IV) data are best fit by inclusion of six Mn−N/O interactions at 1.99 Å, with additional outer-shell contributions from the porphyrin ring. A fit that included only five Mn−N/O interactions gave an essentially identical error value; however, the increased coordination is supported by the decreased pre-edge intensity relative to the Mn(III) complex. The first shell could not be split into two components. A plausible trans axial ligand bound to a Mn(IV) ion is *m*-chlorobenzoate (*m*-CBA), derived from *m*-CPBA, which has been used to generate the Mn(IV)−oxo porphyrin complex (vide infra).

The $[Mn^V(TDCPP)(O)]^+$ complex (**1a**) is best fit by two Mn−O interactions at 1.68 Å and four Mn−N interactions at 2.04 Å, with additional outer-shell contributions from the porphyrin. Inclusion of only a single Mn−O at 1.68 Å results in a significant increase in the error (from 0.60 to 0.99). The larger Debye−Waller value on this component (as compared to the four Mn−N interactions at 2.04 Å) may suggest that the two trans axial Mn−O interactions are at slightly different distances; however, their separation is beyond the resolution limits of the data. The absence of the 1.68 Å Mn−O component gives an error of 3.60 and a significant low-frequency component in the residual. No similar short component can be fit in the Mn(III) or Mn(IV) complexes.

The short Mn−O distances for the $[Mn^V(TDCPP)(O)]^+$ complex (**1a**) are 0.13 Å longer than the Mn−O distances in the five-coordinate $Na[Mn^V(O)(HMPAB)]$[19] and other non-porphyrinic Mn(V)−oxo complexes,[10c,14a,c,d,15] which may be attributed to a trans effect due to the presence of the sixth ligand. Qualitatively, the increase in distance is consistent with the change in Mn−O stretching frequency from the resonance Raman data. However, quantitatively, Badger's rule would predict an even larger change in distance (1.80 Å based on the change in frequency) than is observed.[21] Density functional theory (DFT) calculations on **1a**, both with and without a trans axial ligand, are currently in progress to understand the correlation between the EXAFS-derived distances and the experimental frequencies.

In summary, we have prepared manganese(V)−oxo porphyrins in organic solvents and characterized their physical properties with various spectroscopic techniques. The manganese(V)−oxo porphyrins are diamagnetic low-spin ($S = 0$) species, as characterized by EPR and ^{1}H and ^{19}F NMR spectroscopies. The Mn−O stretching frequency and the Mn−O bond length of **1a**, determined by resonance Raman and X-ray absorption spectroscopy, respectively, are both indicative of a longer, weaker bond than has been observed in previously reported Mn(V)−oxo complexes bearing non-porphyrinic ligands. This suggests double-bond character between the manganese(V) ion and the oxygen atom in porphyrin systems, as indicated by the weak Mn K-pre-edge and the EXAFS data. The weaker Mn−O bond may be attributed to a trans effect due to the presence of a sixth ligand, whereas the previously reported non-porphyrin Mn(V)−oxo complexes are all five-coordinate. More detailed investigations, including DFT calculations, are underway to understand how the ligands of manganese(V)−oxo complexes influence the manganese(V)−oxo bond orders.

Effect of Base on the Stability of Manganese(V)−Oxo Porphyrins. It has been reported previously that the formation of manganese(V)−oxo porphyrins is markedly influenced by the pH of reaction solutions; the intermediates are generated at high pH values in aqueous solution[6,7] or in the presence of base in organic solvents.[9] We therefore investigated the base effect on the generation of manganese(V)−oxo porphyrins by carrying out reactions with Mn(TDCPP)Cl and *m*-CPBA in the presence of different amounts of TBAH. When Mn(TDCPP)Cl was reacted with *m*-CPBA in the absence of TBAH in a solvent mixture of CH_2Cl_2 and CH_3CN (1:1) at 25 °C, $(TDCPP)Mn^{IV}$═O (**2a**) was generated (see Supporting Information, Figure S4 for the UV−vis and EPR spectra of **2a**).[6,7,22] In the presence of 10 equiv of TBAH, **1a** was formed but quickly disappeared, and the decay of **1a** became slower with the increase of TBAH concentration (Supporting Information, Figure S5). Moreover, when 10 equiv of $HClO_4$ was added to a solution of **1a** which was generated in the presence of 20 equiv of TBAH, the intermediate immediately reverted back to the starting $[Mn^{III}(TDCPP)]^+$ complex. These results demonstrate that the role of base is to stabilize manganese(V)−oxo porphyrins. Although we do not know the exact role of base in increasing the stability of manganese(V)−oxo species, the reactivity of manganese(V)−oxo complexes may be controlled by binding the hydroxide ion as an axial ligand (i.e., axial ligand effect).[23] The presence of a sixth trans axial ligand in the Mn(V) complex is supported by the XAS results (vide supra).

(21) (a) Badger, R. M. *J. Chem. Phys.* **1934**, *2*, 128−131. (b) Herschbach, D. R.; Laurie,V. W. *J. Chem. Phys.* **1961**, *35*, 458−463.
(22) (a) Groves, J. T.; Stern, M. K. *J. Am. Chem. Soc.* **1988**, *110*, 8628−8638. (b) Arasasingham, R. D.; He, G.-X.; Bruice, T. C. *J. Am. Chem. Soc.* **1993**, *115*, 7985−7991. (c) Ayougou, K. Bill, E.; Charnock, J. M.; Garner, C. D.; Mandon, D.; Trautwein, A. X.; Weiss, R.; Winkler, H. *Angew. Chem., Int. Ed. Engl.* **1995**, *34*, 343−346.
(23) (a) Meunier, B.; Guilmet, E.; De, Carvalho, M.-E.; Poilblanc, R. *J. Am. Chem. Soc.* **1984**, *106*, 6668−6676. (b) Battioni, P.; Renaud, J. P.; Bartoli, J. F.; Reina-Artiles, M.; Fort, M.; Mansuy, D. *J. Am. Chem. Soc.* **1988**, *110*, 8462−8470. (c) Collman, J. P.; Tanaka, H.; Hembre, R. T.; Brauman, J. I. *J. Am. Chem. Soc.* **1990**, *112*, 3689−3690.

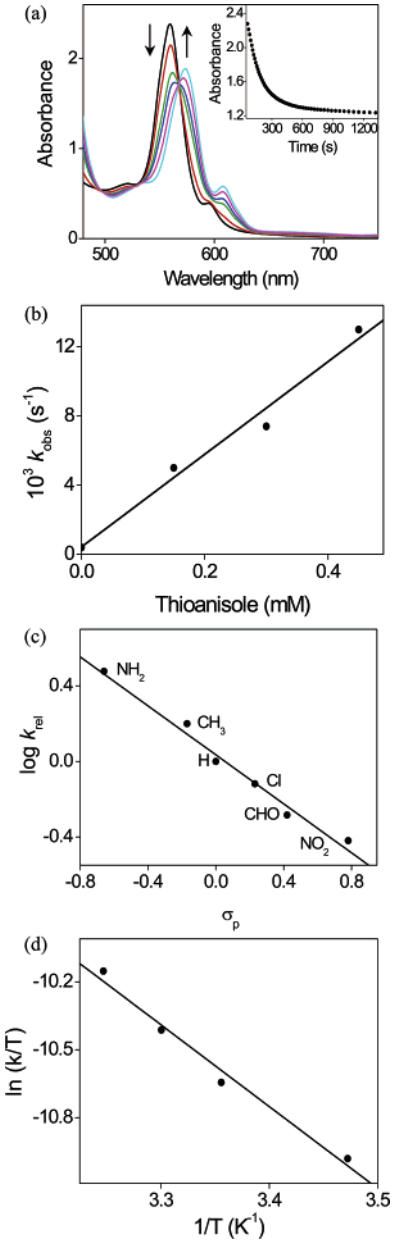

Figure 7. (a) UV−vis spectral changes of **1a** (1.5 mM) upon addition of 100 equiv of thioanisole at 35 °C. Inset shows absorbance traces monitored at 560 nm. (b) Plot of k_{obs} against thioanisole concentration to determine a second-order rate constant. (c) Hammett plot of log k_{rel} against σ_p of thioanisoles in the reactions of **1a** (1.5 mM) and para-X-substituted thioanisoles (10 equiv to **1a**) at 35 °C. (d) Plot of first-order-rate constants against $1/T$ to determine activation parameters.

Reactivities of Manganese(V)−Oxo Porphyrins. We have shown above that manganese(V)−oxo porphyrins are highly stable in the presence of base; **1a** decays slowly with a rate constant of $4.6(4) \times 10^{-4}$ s^{-1} at 35 °C (Table 1). This rate was not dependent on the concentration of [(Porp)Mn^{V}=O]$^{+}$ species. However, the decay rate of manganese(V)−oxo porphyrins was dependent on the nature of the porphyrin ligands; electron-rich manganese porphyrins decayed faster than electron-deficient manganese porphyrins (Table 1 lists k_{obs} values for the decay of manganese(V)−oxo porphyrins).[6b] It is of interest to note that the stability order of manganese(V)−oxo porphyrins is opposite to that of iron(IV)−oxo porphyrin π-cation radicals. In iron porphyrins, an iron(IV)−oxo porphyrin π-cation radical

Scheme 1. Oxygen Exchange between Mn(V)−Oxo Species and $H_2{}^{18}O$

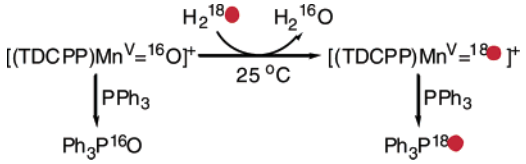

bearing an electron-rich porphyrin ligand is more stable than one bearing an electron-deficient porphyrin.[4d,24] Further, the stability order of manganese(V)−oxo porphyrins in the presence of base is opposite to the reactivity and stability order of [(Porp)Mn^{V}=O]$^{+}$ complexes observed in the absence of base but similar to that of (Porp)Mn^{IV}=O species.[8b] In the latter case, the inverted stability order of manganese(IV)−oxo porphyrins was correlated with ease of the disproportionation of (Porp)Mn^{IV}=O to [Mn^{III}(Porp)]$^{+}$ and [(Porp)Mn^{V}=O]$^{+}$ species.[8b,13]

We then investigated the reactivity of **1a** in oxygen-atom-transfer reactions with various substrates, such as triphenylphosphine (PPh_3), thioanisole ($C_6H_5SCH_3$), cyclooctene, and cyclooctane at 35 °C. Upon addition of 20 equiv of PPh_3 to the solution of **1a** at 35 °C, the intermediate reverted back to the starting [Mn^{III}(TDCPP)]$^{+}$ complex immediately, and product analysis of the resulting solution revealed that Ph_3PO was produced quantitatively. With thioanisole, **1a** reverted back to the starting complex, showing isosbestic points at 496 and 568 nm (Figure 7a). Pseudo-first-order fitting of the kinetic data allowed us to determine the k_{obs} value to be 7.5×10^{-3} s^{-1} at 35 °C. The pseudo-first-order rate constants increased proportionally with thioanisole concentration, giving a second-order rate constant of $2.6(8) \times 10^{-2}$ M^{-1} s^{-1} (Figure 7b). When pseudo-first-order rate constants were determined with various para-substituted thioanisoles and plotted against σ_p, a good correlation was observed, with Hammett ρ value of −0.65 (Figure 7c). The negative ρ value indicates the electrophilic character of the oxo group of **1a** in oxygen-atom-transfer reactions.[25] Further, by determining rate constants from 283 to 308 K, we were able to calculate activation parameters of $\Delta H^{\ddagger} = 7(2)$ kcal mol^{-1} and $\Delta S^{\ddagger} = -44(2)$ cal mol^{-1} K^{-1} for the oxidation of *p*-NH_2-thioanisole by **1a** (Figure 7d).

When the reactivity of **1a** was examined in olefin epoxidation and alkane hydroxylation, the rate of the disappearance of **1a** was not affected by the addition of cyclooctene and cyclooctane to reaction solutions. Further, product analyses revealed that no oxygenated products were generated in these reactions, indicating that **1a** is not capable of oxygenating olefins and alkanes under these conditions. These results are of interest since it has been generally believed that manganese(V)−oxo porphyrin complexes are highly reactive and the sole reactive species in the catalytic oxygenation of olefins and alkanes by manganese(III) porphyrins and terminal oxidants.[5] The low reactivity of **1a** observed in the present study may be ascribed to the binding of an anionic axial ligand (i.e., OH^-) that would serve

(24) Dolphin, D.; Traylor, T. G.; Xie, L. Y. *Acc. Chem. Res.* **1997**, *30*, 251−259.
(25) (a) McPherson, L. D.; Drees, M.; Khan, S. I.; Strassner, T.; Abu-Omar, M. M. *Inorg. Chem.* **2004**, *43*, 4036−4050. (b) Abu-Omar, M. M. *Chem. Commun.* **2003**, 2102−2111. (c) Sivasubramanian, V. K.; Ganesan, M.; Rajagopal, S.; Ramaraj, R. *J. Org. Chem.* **2002**, *67*, 1506−1514.
(26) (a) Meunier, B.; Bernadou, J. *Struct. Bonding.* **2000**, *97*, 1−35. (b) Bernadou, J.; Meunier, B. *Chem. Commun.* **1998**, 2167−2173. (c) Bernadou, J.; Fabiano, A.-S.; Robert, A.; Meunier, B. *J. Am. Chem. Soc.* **1994**, *116*, 9375−9376.

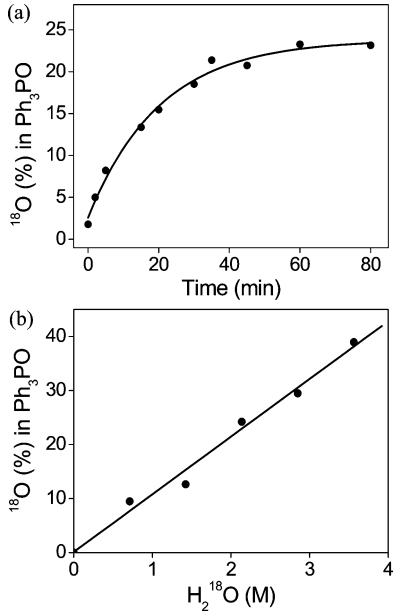

Figure 8. Plots of ^{18}O (%) in Ph_3PO against (a) incubation time and (b) concentration of $H_2{}^{18}O$ for the oxygen exchange between **1a** and $H_2{}^{18}O$. Reaction conditions: (a) **1a** (1.5 mM) was incubated with $H_2{}^{18}O$ (1.4 M, 6 μL of 95% ^{18}O-enriched) in the presence of TBAH (30 mM) in a solvent mixture (0.4 mL) of CH_2Cl_2 and CH_3CN (1:1) at 25 °C. (b) Incubation time was 15 min with different amounts of $H_2{}^{18}O$.

to decrease the electrophilicity of the Mn−oxo complex toward organic substrates (vide infra).

We have also investigated the oxygen exchange between the oxo group of **1a** and $H_2{}^{18}O$ by incubating **1a** in the presence of $H_2{}^{18}O$ and then adding PPh_3 to the resulting solution.[26,27] The degree of ^{18}O exchange was then determined by analyzing ^{16}O and ^{18}O percentages in Ph_3PO product (Scheme 1). Figure 8a shows that the amounts of ^{18}O found in the Ph_3PO product increased with the incubation time of **1a** (see Supporting Information, Figure S6 for the analysis of ^{18}O % in Ph_3PO). Figure 8b shows that the amounts of ^{18}O incorporated into the product increased proportionally with the amounts of $H_2{}^{18}O$ in reaction solutions. The present results provide direct evidence that manganese(V)−oxo porphyrins exchange their oxygen atom with $H_2{}^{18}O$.[6a,7] Interestingly, we found that the rate of oxygen exchange between manganese(V)−oxo porphyrins and $H_2{}^{18}O$ was extremely slow under the reaction conditions; the calculated k_{obs} value of $4.9(2) \times 10^{-2}$ s^{-1} determined in the presence of base in organic solvents at 25 °C is much slower than the estimated rate ($k_{exchange} \approx 10^3$ s^{-1}) of oxo−aqua interchange in an manganese(V)−oxo porphyrin in aqueous solution.[6a]

Catalytic Oxygenation of Olefins and Alkanes by Manganese(V)−Oxo Porphyrins and PhIO. We have used manganese(V)−oxo porphyrins as catalysts in olefin epoxidation and alkane hydroxylation by PhIO. We first generated **1a** by reacting Mn(TDCPP)Cl with *m*-CPBA in the presence of 20 equiv of TBAH. Organic substrates were then added to the reaction solution, followed by solid PhIO (20 equiv). While the UV−vis spectrum of **1a** was retained during the reaction, product analysis of the reaction mixture revealed that epoxides and alcohols were produced in the olefin epoxidation and alkane hydroxylation, respectively (Table 3). In the epoxidation of cyclohexene, cyclohexene oxide was produced predominantly, with small amounts of allylic oxidation products such as cyclohexenol and cyclohexenone (entry 1). In *cis*-stilbene epoxidation, *cis*-stilbene oxide was the major product, with the formation of small amounts of *trans*-stilbene oxide and benzaldehyde (entry 3). This result indicates that the olefin epoxidation is stereospecific, as reported in the epoxidation of *cis*-stilbene by Mn(TDCPP)Cl and PhIO.[28] Also, as observed in the iron porphyrin-catalyzed epoxidation of *trans*-stilbene by PhIO,[29] only a small amount of *trans*-stilbene oxide was produced in the epoxidation of *trans*-stilbene (entry 4). In the hydroxylation of alkanes by **1a** and PhIO, equimolar amounts of alcohol and ketone products were produced (entries 5 and 6).

Table 3. Catalytic Oxygenation of Hydrocarbons by **1a** and PhIO[a]

entry	substrate	product	yield (%)[b,c]
1	cyclohexene	cyclohexene oxide	24 ± 4
		cyclohexenol	2 ± 1
		cyclohexenone	3 ± 1
2	cyclooctene	cyclooctene oxide	36 ± 4
3	*cis*-stilbene	*cis*-stilbene oxide	27 ± 4
		trans-stilbene oxide	3 ± 1
		benzaldehyde	2 ± 1
4	*trans*-stilbene	*trans*-stilbene oxide	4 ± 1
		benzaldehyde	2 ± 1
5	cyclohexane	cyclohexanol	10 ± 3
		cyclohexanone	9 ± 3
6	cyclooctane	cyclooctanol	16 ± 4
		cyclooctanone	13 ± 3

[a] Reactions were run at least in triplicate, and the data reported represent the average of these reactions. See Experimental Section for detailed reaction conditions. [b] Yields were determined on the basis of the amounts of PhIO added. [c] No formation of oxygenated products was detected in the absence of the manganese catalyst.

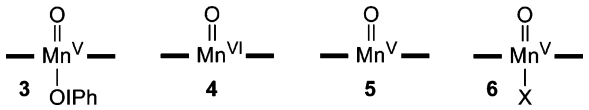

Figure 9. Plausible intermediates involved in the oxygenation of hydrocarbons by [(Porp)Mn^{V}=O]$^+$ and PhIO.

Since we have demonstrated above that **1a** does not oxygenate olefins and alkanes, the observation of the formation of oxygenated products in the catalytic olefin epoxidation and alkane hydroxylation by **1a** and PhIO implies the generation of an active oxidant that is different from **1a**. Similar to the present results, it has been reported previously that manganese(V)−oxo complexes of corrolazine and corrole ligands are inactive, but the Mn(V)−oxo complexes produce oxygenated products in the oxidation of olefins and sulfides by PhIO.[10a,11b] Figure 9 depicts plausible oxidants that may be involved in the oxygenation reactions by **1a** and PhIO. Those are (Porp)Mn^{V}(O)(OIPh) (**3**), [(Porp)Mn^{VI}=O]$^{2+}$ (**4**), [(Porp)Mn^{V}=O]$^+$ with a high-spin Mn(V) state (**5**), and [(Porp)Mn^{V}=O(X)]$^+$ bearing a different axial ligand from **1a** (**6**) (e.g., H_2O). Structure **3**, a PhIO−manganese(V)−oxo adduct, has been frequently suggested as an active oxidant in metal complex-catalyzed oxidation reactions by PhIO, such as in the oxidation of sulfides by (corrolazine)-

(27) (a) Lee, K. A.; Nam, W. *J. Am. Chem. Soc.* **1997**, *119*, 1916−1922. (b) Seo, M. S.; In, J.-H.; Kim, S. O.; Oh, N. Y.; Hong, J.; Kim, J.; Que, L., Jr.; Nam, W. *Angew. Chem., Int. Ed.* **2004**, *43*, 2417−2420. (c) Song, W. J.; Sun, Y. J.; Choi, S. K.; Nam, W. *Chem. Eur. J.* **2006**, *12*, 130−137.

(28) Park, S.-E.; Song, W. J.; Ryu, Y. O.; Lim, M. H.; Song, R.; Kim, K. M.; Nam, W. *J. Inorg. Biochem.* **2005**, *99*, 424−431.

(29) Groves, J. T.; Nemo, T. E. *J. Am. Chem. Soc.* **1983**, *105*, 5786−5791.

Mn(V)═O and PhIO.[10b,30] Structure **4**, a manganese(VI)−oxo porphyrin complex, has not yet been identified, but Golubkov and Gross recently reported the characterization of a (nitrido)-Mn(VI) corrole complex.[31] A high-spin Mn(V)−oxo complex (**5**) has been proposed as an active oxidant on the basis of DFT calculations on a (salen)Mn(V)−oxo intermediate in Jacobsen−Katsuki epoxidation reactions.[32] According to the DFT calculations, manganese(V)−oxo complexes having different spin states (e.g., singlet, triplet, and quintet) show markedly different reactivities in oxidation reactions. Further, Shaik and co-workers conducted DFT calculations with oxoiron(IV) porphyrin π-cation radicals and proposed that the reactivity of the oxoiron(IV) porphyrins is significantly affected by the spin states of the intermediates (i.e., a low-spin doublet state and a high-spin quartet state).[1c,33] Finally, since the low reactivity of **1a** may be due to the binding of hydroxide as an axial ligand, replacement of the axial hydroxide ligand upon addition of PhIO in the catalytic oxygenation reactions could generate an intermediate with high reactivity. Indeed, it has been well documented that the presence of neutral nitrogen bases (e.g., imidazoles) in manganese porphyrin-catalyzed reactions increases product yields dramatically.[34] Therefore, structure **6** may be a Mn(V)−oxo porphyrin complex bearing a different axial ligand (e.g., H_2O). At the present time, none of the proposed species in Figure 9 has been identified, and intensive mechanistic studies are needed to elucidate the exact nature of active oxidant(s) in manganese complex-catalyzed oxidation reactions.

Conclusion

Manganese(V)−oxo species have been frequently invoked as reactive species in the catalytic oxygenation of hydrocarbons by manganese(III) porphyrins and terminal oxidants.[5] In the present study, we have prepared manganese(V)−oxo porphyrins that are highly stable at room temperature in the presence of base in organic solvents. The manganese(V)−oxo porphyrins were characterized with various spectroscopic techniques and found to be diamagnetic low-spin ($S = 0$) species with a longer, weaker Mn−O bond than that found in previously characterized Mn(V)−oxo complexes. This is suggestive of double-bond character between the manganese(V) ion and the oxygen atom and originates from the presence of a sixth trans axial ligand. The stability of the manganese(V)−oxo species was found to depend on the concentration of base and the electronic nature of porphyrin ligands, but not on the concentration of the manganese(V)−oxo species. The low-spin manganese(V)−oxo porphyrins showed a low reactivity in oxygen-atom-transfer reactions;[35] the intermediates are capable of oxygenating PPh_3 and thioanisoles but not olefins and alkanes. Moreover, the rate of oxygen exchange between the manganese(V)−oxo species and $H_2{}^{18}O$ in the presence of base in organic solvents was found to be very slow. These results are in contrast to previous suggestions that manganese(V)−oxo porphyrins are invariably highly reactive in oxygenation reactions and that the intermediates exchange their oxygen with $H_2{}^{18}O$ at a fast rate. We have also reported that manganese(V)−oxo porphyrins associated with terminal oxidants, such as PhIO, afforded high product yields in the oxygenation of olefins and alkanes. Future studies will focus on elucidating the effect(s) of base on the chemical properties of manganese(V)−oxo species and the nature of oxygenating intermediate(s) generated in the reactions of manganese(V)−oxo porphyrins and terminal oxidants.

Experimental Section

Materials. Dichloromethane (anhydrous) and acetonitrile (anhydrous) were obtained from Aldrich Chemical Co. and purified by distillation over CaH_2 prior to use. All reagents purchased from Aldrich were the best available purity and used without further purification unless otherwise indicated. *m*-CPBA was purified by washing with phosphate buffer (pH 7.4) followed by water and then dried under reduced pressure. Iodosylarenes were prepared according to published procedures.[36] The purities of the oxidants were determined by iodometric titration.[37] $H_2{}^{18}O$ (95% ^{18}O-enriched) and $H_2{}^{18}O_2$ (90% ^{18}O-enriched, 2% $H_2{}^{18}O_2$ in water) were purchased from ICON Services Inc. (Summit, NJ). Mn(TDCPP)Cl, Mn(TDFPP)Cl, Mn(TPFPP)Cl, Mn(TMP)Cl, and Mn(TM-2-PyP)Cl_5 were obtained from Mid-Century Chemicals (Posen, IL). Mn(TDMPP)Cl was synthesized according to published procedures.[38]

Instrumentation. UV−vis spectra were recorded on a Hewlett-Packard 8453 spectrophotometer equipped with a circulating water bath. EPR spectra were obtained on a JEOL JES-FA200 spectrometer at 4 K. ^{1}H NMR spectra were measured with a Bruker DPX-250 spectrometer, and chemical shifts were reported as δ values from standard solvent peaks. ^{19}F NMR spectrum was measured with a Varian Unity-Inova 500 MHz spectrometer. Product analyses for the oxidation of PPh_3 and the epoxidation of *cis*- and *trans*-stilbenes were performed on a DIONEX Summit Pump Series P580 equipped with a variable-wavelength UV-200 detector (HPLC). Products were separated on a Waters Symmetry C18 reverse-phase column (4.6 × 250 mm), and detection was made at 215 and 254 nm. Product analyses for the oxidation of sulfides, the epoxidation of cyclohexene and cyclooctene, and the hydroxylation of alkanes were performed on an Agilent Technologies 6890N gas chromatograph equipped with a flame ionization detector (GC) and a Hewlett-Packard 5890 II Plus gas chromatograph interfaced with a Hewlett-Packard model 5989B mass spectrometer (GC−MS). LC-ESI MS spectra for the determination of ^{18}O percentage in Ph_3PO in isotopically labeled $H_2{}^{18}O$ experiments were collected on a Finnigan Surveyor Integrated HPLC system (PDA detector and LC pump) connected with a Thermo Finnigan (San Jose, CA) LCQ Advantage MAX quadrupole ion trap instrument. The separation of product was achieved by on-column injection to a Hypersil GOLD column (5 μm, 4.6 × 250 mm) using MeOH:H_2O (3:1) as eluent

(30) (a) Nam, W.; Ryu, Y. O.; Song, W. J. *J. Biol. Inorg. Chem.* **2004**, *9*, 654−660 and references therein. (b) Mahammed, A.; Gross, Z. *J. Am. Chem. Soc.* **2005**, *127*, 2883−2887. (c) Collman, J. P.; Zeng, L.; Brauman, J. I. *Inorg. Chem.* **2004**, *43*, 2672−2679. (d) Collman, J. P.; Zeng, L.; Decréau, R. A. *Chem. Commun.* **2003**, 2974−2975. (e) Nam, W.; Jin, S. W.; Lim, M. H.; Ryu, J. Y.; Kim, C. *Inorg. Chem.* **2002**, *41*, 3647−3652.
(31) Golubkov, G.; Gross, Z. *J. Am. Chem. Soc.* **2005**, *127*, 3258−3259.
(32) (a) Strassner, T.; Houk, K. N. *Org. Lett.* **1999**, *1*, 419−421. (b) Cavallo, L.; Jacobsen, H. *Eur. J. Inorg. Chem.* **2003**, 892−902. (c) Abashkin, Y. G.; Burt, S. K. *Org. Lett.* **2004**, *6*, 59−62.
(33) (a) Shaik, S. Kumar, D.; de Visser, S. P.; Altun, A.; Thiel, W. *Chem. Rev.* **2005**, *105*, 2279−2328. (b) Shaik, S.; de Visser, S. P.; Kumar, D. *J. Biol. Inorg. Chem.* **2004**, *9*, 661−668.
(34) (a) Lai, T.-S.; Lee, S. K. S.; Yeung, L.-L.; Liu, H.-Y.; Williams, I. D.; Chang, C. K. *Chem. Commun.* **2003**, 620−621. (b) Collman, J. P.; Chien, A. S.; Eberspacher, T. A.; Zhong, M.; Brauman, J. I. *Inorg. Chem.* **2000**, *39*, 4625−4629. (c) Battioni, P.; Renaud, J. P.; Bartoli, J. F.; Reina-Artiles, M.; Fort, M.; Mansuy, D. *J. Am. Chem. Soc.* **1988**, *110*, 8462−8470. (d) Meunier, B.; Guilmet, E.; De, Carvalho, M.-E.; Poilblanc, R. *J. Am. Chem. Soc.* **1984**, *106*, 6668−6676.
(35) It has been suggested from DFT calculations that the reactivity of a low-spin Mn(V)−oxo porphyrin complex is low: de Visser, S. P.; Ogliaro, F.; Gross, Z.; Shaik, S. *Chem. Eur. J.* **2001**, *7*, 4954−4960.
(36) Saltzman, H.; Sharefkin, J. G. *Organic Syntheses;* Wiley: New York, 1973; Collect. Vol. V, p 658.
(37) Lucas, H. J.; Kennedy, E. R.; Formo, M. W. *Organic Syntheses;* Wiley: New York, 1955; Collect. Vol. III, p 483.
(38) Lindsey, J. S.; Wagner, R. W. *J. Org. Chem.* **1989**, *54*, 828−836.

at a flow rate of 1 mL/min, at a spray voltage 4.7 kV and a capillary temperature at 220 °C.

Preparation of Manganese(V)− and Manganese(IV)−Oxo Complexes. In general, **1** (0.15 mM) was prepared by adding 2 equiv of *m*-CPBA (0.3 mM, diluted in 50 μL of CH_3CN) into a 0.1-cm UV cuvette containing a manganese(III) porphyrin chloride (0.15 mM) and TBAH (3.0 mM) in a solvent mixture (0.5 mL) of CH_3CN and CH_2Cl_2 (1:1) at 25 °C. **2** was generated by reacting Mn(TDCPP)Cl with 2 equiv of *m*-CPBA in a solvent mixture (0.5 mL) of CH_3CN and CH_2Cl_2 (1:1) at 25 °C. The formation of **1** and **2** was monitored by a UV−vis spectrophotometer, and the resulting solution was used immediately for further studies.

Resonance Raman Measurements. Samples for resonance Raman were prepared as follows: **1a**-^{16}O was prepared by reacting Mn(TDCPP)Cl (0.4 mM) with *m*-CPBA (0.8 mM) in the presence of TBAH (8 mM) in CH_3CN (0.5 mL) at 10 °C, whereas **1a**-^{18}O was prepared by reacting Mn(TDCPP)Cl (0.4 mM) with $H_2{}^{18}O_2$ (0.8 mM) or exchanging the oxygen atom of **1a**-^{16}O with $H_2{}^{18}O$ (15 μL of 95% ^{18}O-enriched). The $[(TM\text{-}2\text{-}PyP)Mn^{V}{=}{}^{16}O]^{5+}$ and $[(TM\text{-}2\text{-}PyP)Mn^{V}{=}{}^{18}O]^{5+}$ intermediates were prepared by reacting $[Mn^{III}(TM\text{-}2\text{-}PyP)]^{5+}$ (0.4 mM) with $PhI^{16}O$ and $PhI^{18}O$ (0.8 mM, diluted in 10 μL of CH_3OH) in the presence of TBAH (8 mM) in $H_2{}^{16}O$ (0.5 mL) and $H_2{}^{18}O$ (0.5 mL), respectively, at 10 °C. The absence of Mn(IV)−oxo species was confirmed by taking the UV−vis spectra of resonance Raman samples. The samples were transferred in a quartz spinning cell precooled at 10 °C. Resonance Raman spectra were obtained using a liquid-nitrogen-cooled CCD detector (model LN/CCD-1100-PB, Roper Scientific) attached to a 1-m single polychromator (model MC-100DG, Ritsu Oyo Kogaku). An excitation wavelength of 441.6 nm was provided by a He−Cd laser (model CD4805R, Kinmon Electric), with 4 mW power at the samples. All measurements were carried out with a quartz spinning cell (1000 rpm) at ∼10 °C. Raman shifts were calibrated with indene, and the accuracy of the peak positions of the Raman bands was ±1 cm^{-1}.

XAS Data Collection and Analysis. XAS data for Mn^{III}(TDCPP)(OH), Mn^{IV}(TDCPP)(O), and $[Mn^{V}$(TDCPP)(O)$]^+$ (**1a**) were recorded at the Stanford Synchrotron Radiation Laboratory (SSRL) on focused beam line 9-3, under ring conditions of 3 GeV and 80−100 mA. A Si(220) monochromator (fully tuned) was used for energy selection. A Rh-coated mirror (set to a cutoff of 10 keV) was used for harmonic rejection. All XAS samples (∼2 mM) were measured as solutions in CH_3CN. Samples were loaded into 2-mm Delrin XAS cells with Kapton windows and then frozen immediately in liquid nitrogen prior to XAS measurements. During XAS measurements, samples were maintained at a constant temperature of 10 K by an Oxford Instruments CF1208 continuous-flow liquid-helium cryostat.

Data were measured in fluorescence mode using a Canberra Ge 30-element array detector. XAS data were measured to $k = 11$ Å^{-1} due to contributions from both Fe contamination and diffraction (resulting from a poor glass). Internal energy calibration was performed by simultaneous measurement of the absorption of a Mn foil placed between the second and third ionization chambers. The first inflection point of the Mn foil was assigned to 6539.0 eV. Samples were monitored for photoreduction throughout the course of data collection. Only those scans which showed no evidence of photoreduction were used in the final average. The data represent eight, six, and six scan averages for the Mn^{III}(TDCPP)(OH), Mn^{IV}(TDCPP)(O), and $[Mn^{V}$(TDCPP)(O)$]^+$ complexes, respectively.

The averaged data were processed as described previously[39] by fitting a second-order polynomial to the post-edge region and subtracting this background from the entire spectrum. A three-region cubic spline was used to model the smooth background above the edge. Normalization of the data was achieved by subtracting the spline and normalizing the post-edge region to 1. The resultant EXAFS was k^3-weighted to enhance the impact of high-*k* data.

Theoretical EXAFS signals $\chi(k)$ were calculated using FEFF (version 7.0)[40] and fit to the data using EXAFSPAK.[41] The non-structural parameter E_0 was also allowed to vary but was restricted to a common value for every component in a given fit. The structural parameters varied during the refinements were the bond distance (R) and the bond variance (σ^2). σ^2 is related to the Debye−Waller factor, which is a measure of thermal vibration and static disorder of the absorbers/scatters. Coordination numbers were systematically varied in the course of the analysis, but they were not allowed to vary within a given fit. Single scattering paths and the corresponding multiple scattering paths were linked during the course of refinements.

Reactions of $[(TDCPP)Mn^{V}{=}O]^+$ (1a) with Organic Substrates. All reactions were run in a 0.1-cm UV cuvette by monitoring UV−vis spectral changes of reaction solutions. **1a** was prepared by reacting Mn^{III}(TDCPP)Cl (1.5 mM) with 2 equiv of *m*-CPBA (3 mM) in the presence of TBAH (30 mM) in a solvent mixture (0.4 mL) of CH_2Cl_2/CH_3CN (1:1) at 35 °C. Substrate (0.15 M) was then added to the solution of **1a**. After the completion of the reaction, the reaction mixture was directly analyzed by HPLC, GC, and/or GC−MS. Product yields were determined by comparison against standard curves prepared with known authentic samples.

The labeled water ($H_2{}^{18}O$) experiments for oxygen exchange between **1a** and $H_2{}^{18}O$ were carried out as follows: **1a** was prepared as described above. Appropriate amounts of $H_2{}^{18}O$ (95% ^{18}O-enriched) were then added to the solution of **1a**, followed by incubation of the resulting solution for the given time. After addition of PPh_3 (0.15 M) to the solution of **1a**, the ^{18}O percentage in the Ph_3PO product was determined by analyzing reaction solutions with LC-ESI MS, and the ^{16}O and ^{18}O compositions in the Ph_3PO product were analyzed by the relative abundances of $m/z = 279.2$ for $[Ph_3P^{16}O + H^+]^+$ and $m/z = 281.2$ for $[Ph_3P^{18}O + H^+]^+$.

Catalytic Oxygenation of Organic Substrates by 1a and PhIO. **1a** was prepared by reacting Mn^{III}(TDCPP)Cl (1.5 mM) with 2 equiv of *m*-CPBA (3 mM) in the presence of TBAH (30 mM) in a solvent mixture (0.5 mL) of CH_2Cl_2/CH_3CN (1:1) at 25 °C. Substrate (0.15 M, diluted in CH_2Cl_2/CH_3CN (1:1)) was added to the reaction solution, followed by the addition of solid PhIO (20 equiv to the catalyst). For comparison, control experiments were carried out in the absence of the manganese catalyst in the oxidation of cyclohexene and cyclohexane. After the solid PhIO disappeared completely (ca. 2 h), the resulting solution was directly analyzed by GC, HPLC, and/or GC−MS. Product yields were determined by comparison against standard curves prepared with known authentic samples.

Acknowledgment. This research was supported by the Ministry of Science and Technology of Korea through Creative Research Initiative Program (to W.N.), the Korea Research Foundation (KRF-2005-217-C00006 to M.S.S.), the BK 21 Program (to M.-J.K.), Grant-in-Aid from the Ministry of Education, Culture, Sports, Science and Technology, Japan (14001004 to T.K.), and a JSPS Research Fellowship for Young Scientists (to T.O. and T.T.). SSRL operations are funded by the U.S. Department of Energy, Office of Basic Energy Sciences. The Structural Molecular Biology program is supported by the National Institutes of Health, National Center for Research Resources, Biomedical Technology Program, and by

(39) DeWitt, J. G.; Bentsen, J. G.; Rosenzweig, A. C.; Hedman, B.; Green, J.; Pilkington, S.; Papaefthymiou, G. C.; Dalton, H.; Hodgson, K. O.; Lippard, S. J. *J. Am. Chem. Soc.* **1991**, *113*, 9219−9235.

(40) (a) Rehr, J. J.; Mustre de Leon, J.; Zabinsky, S. I.; Albers, R. C. *J. Am. Chem. Soc.* **1991**, *113*, 5135−5140. (b) Mustre de Leon, J.; Rehr, J. J.; Zabinsky, S. I.; Albers, R. C. *Phys. Rev. B* **1991**, *44*, 4146−4156.

(41) George, G. N. EXAFSPAK & EDG_FIT, 2000, Stanford Synchrotron Radiation Laboratory, Stanford Linear Accelerator Center, Stanford University, Stanford, CA 94309.

the Department of Energy, Office of Biological and Environmental Research. We thank Prof. James E. Penner-Hahn (University of Michigan) for providing the Mn K-edge data of Na[Mn^{V}(HMPAB)(O)].

Supporting Information Available: UV−vis spectra of [(Porp)Mn^{V}═O]$^{+}$ complexes (Figure S1), ^{1}H and ^{19}F NMR spectra of [(TDFPP)Mn^{V}═O]$^{+}$ (Figure S2), UV−vis spectrum of (TM-2-PyP)Mn^{V}═O (Figure S3), UV−vis and EPR spectra of (TDCPP)Mn^{IV}═O (**2a**) (Figure S4), time traces for the natural decay of **1a** in the presence of different amounts of base (Figure S5), and LC-ESI MS of PPh_3O obtained in isotope labeling experiment (Figure S6). This material is available free of charge via the Internet at http://pubs.acs.org.

JA066460V